IOP PUBLISHING NONLINEARITY

Nonlinearity **22** (2009) 2845–2859 doi:10.1088/0951-7715/22/12/003

A delay model for noise-induced bi-directional switching*

Jinzhi Lei[1], **Guowei He**[2], **Haoping Liu**[3,6] **and Qing Nie**[4,5,6]

[1] Zhou Pei-Yuan Center for Applied Mathematics, Tsinghua University, Beijing 100084, People's Republic of China
[2] LNM, Institute of Mechanics, Chinese Academy of Sciences, Beijing 100080, People's Republic of China
[3] Department of Biological Chemistry, School of Medicine, University of California, Irvine, CA 92697, USA
[4] Department of Mathematics, University of California, Irvine, CA 92697, USA
[5] Center for Mathematical and Computational Biology, University of California, Irvine, CA 92697, USA
[6] Center for Complex Biological Systems, University of California, Irvine, CA 92697, USA

E-mail: qnie@math.uci.edu

Received 22 June 2009, in final form 3 October 2009
Published 30 October 2009
Online at stacks.iop.org/Non/22/2845

Recommended by A L Bertozzi

Abstract

Many biological systems can switch between two distinct states. Once switched, the system remains stable for a period of time and may switch back to its original state. A gene network with bistability is usually required for the switching and stochastic effect in the gene expression may induce such switching. A typical bistable system allows one-directional switching, in which the switch from the low state to the high state or from the high state to the low state occurs under different conditions. It is usually difficult to enable bi-directional switching such that the two switches can occur under the same condition. Here, we present a model consisting of standard positive feedback loops and an extra negative feedback loop with a time delay to study its capability to produce bi-directional switching induced by noise. We find that the time delay in the negative feedback is critical for robust bi-directional switching and the length of delay affects its switching frequency.

Mathematics Subject Classification: 92B05, 34K50, 92D10

(Some figures in this article are in colour only in the electronic version)

* This paper is published as part of a collection in honour of Todd Dupont's 65th birthday.

1. Introduction

Living cells can switch from one fate to another during growth, development and regeneration. In unicellular organisms switching between different phenotypes is important for better survival and adaptation to the ever-changing host environment [1, 36, 45, 49]. Once a cell switches, it remains stable, acting as a cellular memory unit [16, 20, 50]. It becomes increasingly clear that stochasticity in gene expression in conjunction with the architecture of the gene network that underlies the cellular processes can generate such phenotypic variation and switching [14, 21–23, 29, 33, 34, 37, 40, 46]. The underlying molecular mechanisms responsible for such an event usually involve positive feedback loops and/or double-negative feedback loops, because of their capability to produce bistability and switching responses in gene regulation [5, 10–12, 15, 16, 28, 32, 38, 47].

For example, in *Escherichia coli*, a genetic toggle switch, which was a synthetic, bistable gene-regulatory network constructed from any two repressible promoters arranged in a mutually inhibitory network, could be flipped between two stable states [16]. In *Saccharomyces cerevisiae*, an engineered cell strain can randomly switch between two cell phenotypes as a result of stochastic gene expression [1]. *Candida albicans*, one of the fungi, can reversibly switch between two visibly different cell types, white and opaque cells [35, 41–43]. White-phase cells appear relatively round and they express a set of white-specific genes. Opaque cells are larger and more elongated and they express a set of opaque-specific genes [43]. The opaque-phase cells are more virulent in cutaneous models of infection, and white-phase cells are more virulent in systemic infection [7, 25, 48]. Although the molecular mechanisms responsible for white-opaque switching and for the heritability of the white and opaque states are not yet fully understood, recently *wor1* (white-opaque regulator 1) has been identified as the master regulator of white-opaque switching [20, 52]. WOR1 expression shows an all-or-none pattern in single cell. It is not detectable in white cells and is highly expressed in opaque cells. In particular, WOR1 forms a positive feedback loop by binding to its own promoter and activates its own transcription [52].

The mathematical models on switching of cell phenotype primarily focus on modelling the regulatory network that induces the gene expression from one state to another state [19, 47]. The switching may occur because of an external stimulus that can be converted into all-to-none response [6, 16, 32, 51] or due to internal sources, such as the stochasticity in gene expression [19, 44, 47]. Noise (e.g. in gene expression) has been found to be a critical factor to destabilize one state to induce switching [19]. From the modelling point of view, the noise-induced switching mechanism is achieved as the noise enables kinetic parameters to move from one stability region to another stability region. In other words, a bi-stable system shifts to another stable steady state from its current state. This mechanism requires the control kinetic parameter, which is affected by noise, must be near the critical values of the stability region, and it makes difficult for a system to be able to switch between two stable states under the same set of parameters and the same level of noise effects.

In this paper, motivated by the white-opaque switch in *Candida albicans*, we present a model that allows robust switching between two stable states under the same set of parameters (a bi-directional switching). The model includes a combination of fast positive feedback loops and a negative feedback with a time delay. Through simulation and analysis, we first show that the system with the positive feedback alone cannot induce any bi-directional switches unless the kinetic parameters are fine-tuned into a narrow range and the noise is unrealistically strong. Next, we demonstrate that adding a negative feedback loop with large lag time can destabilize the high state and induce bi-directional switching through noise effect between the low and high states. The dynamics of the switching and the switching frequency are also discussed.

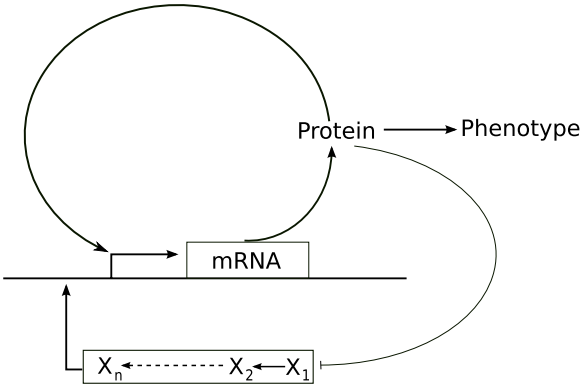

Figure 1. Illustration of a gene regulation network with a delay for bi-directional switching. In the system, the protein can bind to its own promoter to activate the expression forming a positive feedback as well as inhibit the expression indirectly through many other genes.

2. Model formulation

In the model, the cell phenotype is assumed to be determined by the expression level of a master gene (see in figure 1). A positive feedback functions through the protein binding to its own promoter to further activate the gene expression, as the case for many systems with bi-stability [3, 15, 16, 19, 28, 32, 47]. In the system, we also assume that the protein may negatively regulate the master gene expression through many steps of regulation of some downstream genes (illustrated by $X_1, \ldots, X_n$ in figure 1). Delays usually occur for such negative regulations, compared with the direct regulation such as the positive regulation in the system, due to time needed for gene transcriptions, transport of the associated proteins and regulation of a cascade of downstream transcriptions. To simplify the model, we lump these steps as one negative feedback with a *delay* from the protein to the gene expression. A similar approach was used in a study of the intracellular circadian rhythm generator [31], in which a delay term was introduced to represent a cascade of actions in a feedback loop including translation and protein synthesis.

Denote x as the protein concentration and y as the mRNA concentration of the master gene. The protein is translated from mRNA, which is synthesized through the transcription of the gene. The transcriptional rate is proportional to the promoter activity that depends on the concentration of protein (x) and the negative regulation loop (i.e. through X_n in figure 1). The concentration of X_n in turn depends on the history of $x(t)$, i.e. $x(t-\tau)$ with τ being the lag time for the intermediate genes at work. Accordingly, the dynamics of the model described in figure 1 can be written in terms of the following delay differential equations:

$$\begin{aligned} \tau_x \frac{\mathrm{d}x}{\mathrm{d}t} &= \beta y - x, \\ \tau_y \frac{\mathrm{d}y}{\mathrm{d}t} &= \alpha h_0(x) h_1(x_\tau) - y. \end{aligned} \tag{1}$$

Here x_τ stands for $x(t-\tau)$, and $h_0(x)$ and $h_0(x)$ are the Hill functions modelling the feedbacks:

$$h_0(x) = \rho_0 + (1-\rho_0)\frac{(x/\theta_0)^{n_0}}{1+(x/\theta_0)^{n_0}}, \tag{2}$$

$$h_1(x) = \rho_1 + (1-\rho_1)\frac{1}{1+(x/\theta_1)^{n_1}}. \tag{3}$$

Here, ρ_i represents the ratio between the lowest promoter activity and the highest promoter activity, and it takes values from 0 to 1. When $\rho_i = 1$, then $h_i(x) \equiv 1$ implying no feedback regulation. Therefore ρ_i is referred to as the effectiveness of the corresponding feedback, e.g. smaller ρ_i implying stronger feedback regulation. The parameters θ_i ($i = 0, 1$) are 50% effective concentration (EC50) of the feedback loops. With a suitable unit for the concentration, one can assume one of the EC50s, say θ_0, equals 1. Consequently, x, y and θ_1 measure the concentrations with respect to θ_0, respectively. The exponents n_0 and n_1 in (2) and (3) are the Hill coefficients that measure the steepness of the response in the Hill function. They are usually related to the number of binding sites in the promoter that interact with the protein [2], and a reaction with the Hill coefficient $n > 1$ is often referred to as *cooperative* reaction. The cooperative reaction is usually required for achieving bistable expressions [9, 16, 32]. In this paper, we will take $n_0 = n_1 = 2$.

In this formulation, the transcriptional rate of mRNA depends on the protein level through the product of two Hill functions: an increasing function of x for the positive feedback and a decreasing function of x_τ for the negative feedback with delay time τ. The transcriptional rate of mRNA depends on the protein concentration with a maximal value α. The parameter β measures the average number of proteins produced by each mRNA, termed as *translational efficiency*. The proteins and mRNA are depleted in a first-order reaction with time constants τ_x and τ_y, respectively.

The extrinsic noise effect due to environment and system variability may be modelled through the randomness of the two rate constants α and β in (1) [26, 39]. Here, we consider only the noise perturbation to the translational efficiency β, and replace β by a log-normal distribution noisy rate [4, 39]

$$\bar{\beta}_\xi(t) = \beta \mathrm{e}^{\sigma\xi(t)} / \langle \mathrm{e}^{\sigma\xi(t)} \rangle, \tag{4}$$

where $\xi(t)$ is a standard white noise, and $\sigma > 0$ is a constant to indicate the perturbation strength. The exponentiating $\sigma\xi(t)$ ensures a positive $\bar{\beta}_\xi(t)$. Log-normal rather than normal distribution has been measured for gene expression rates [4].

In summary, the equation for the model described in figure 1 with the extrinsic noise on the translational efficiency takes the form

$$\begin{aligned} \tau_x \frac{\mathrm{d}x}{\mathrm{d}t} &= \bar{\beta}_\xi(t) y - x, \\ \tau_y \frac{\mathrm{d}y}{\mathrm{d}t} &= \alpha h_0(x) h_1(x_\tau) - y. \end{aligned} \tag{5}$$

Here $\bar{\beta}_\xi(t)$ depends on the white noise $\xi(t)$ according to (4). Next, we investigate bistability, the effect of delay and bi-directional switching of the above system.

3. Result

3.1. Noise-induced switching in the system with only a positive feedback

Here, we consider the case in which the indirect negative feedback loop is turned off by setting $\rho_1 = 1$ in equation (5), i.e. $h_1(x) \equiv 1$. First, we study the condition under which bistability of the protein level occurs when the noise is absent (i.e. $\bar{\beta}_\xi(t) \equiv \beta$). The corresponding steady state concentrations of protein and mRNA, denoted by (x^*, y^*), are positive solutions of the equation.

$$y^* = \alpha h_0(\beta y^*) \qquad x^* = \beta y^*. \tag{6}$$

Figure 2(*a*) plots three parameter regions for the system to achieve (1) monostable state at the high protein level or the low protein level and (2) bistable states like figure 2(*b*), which

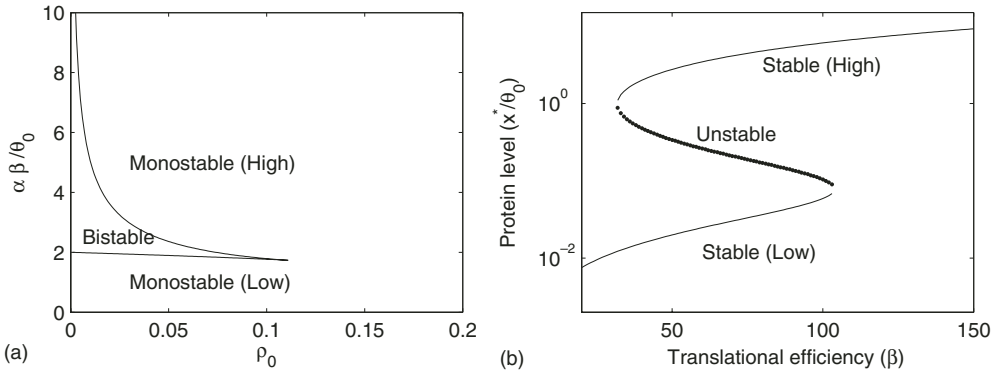

Figure 2. Bistability of the model with the positive feedback alone. (*a*) Parameter regions for bistable expression; (*b*) the protein level normalized by the EC50 (x^*/θ_0) at steady state as a function of translational efficiency (β). In the simulation, $\alpha = 0.0625$, $\rho_0 = 0.006$, $\rho_1 = 1.9$, $n_0 = 2$.

plots a bistable dependence of protein level (x^*/θ_0) on the translational efficiency β. As seen from figure 2(*a*), the bistable expression occurs only when $\rho_0 < 0.1$ and $\alpha\beta/x_0$, the maximal level of proteins with respect to the EC50 of the positive feedback, takes an intermediate value. For example, when $\rho_0 = 0.006$, one needs $2 < \alpha\beta/x_0 < 6.5$ to ensure the bistable expression. For bacteria, the average number of proteins produced by each mRNA was estimated to be $60 < \beta < 110$ [17], then we need to require $0.045 < \alpha < 0.083$ if the EC50 $\theta_0 = 1$ by a suitable unit for the concentration. In the simulations, we take $\alpha = 0.0625$, a value around the middle of the range.

Figure 2(*b*) shows the protein level normalized by the EC50 (x^*/θ_0) at steady state as a function of translational efficiency (β) . When $32 < \beta < 103$, the cell has bistable expression of the master gene (figure 2).

When the system is bistable with one stable low state and one stable high state, a noise-induced perturbation to the gene expression has been thought to be able to induce the switching between the two states [47, 52]. To study whether noise can robustly induce the reliable switches, we numerically simulate system (5) (with $h_1 \equiv 1$) for various translational efficiencies.

In each simulation, we set the initial concentrations of protein level and mRNA at their stable steady state solution level of the corresponding deterministic equations, and the solution is computed up to the time of 10 h. To mimic the biological systems, we denote $x(t = 10\,\text{h})$ as the state (or phenotype) of the solution, and denote each solution as one cell. Figure 3(*a*) plots the distribution of cells at different states at time of 10 h, starting with cells either at the low state (lower panel) or the high state (upper panel), for a range of values of the translational efficiency β.

As shown in figure 3(*a*), the cell initially at the high state can switch to the low state when $32 < \beta < 54$ (upper panel) and the cell initially at the low state can switch to the high state when $46 < \beta < 103$ (low panel), due to noises. It is found from the simulations that the range of β ensuring the switching from the low to the high state is larger than that for the switching from the high to the low state, suggesting that the switching from the low state to the high state may be more robust than the switching from the high state to the low state.

From figure 3(*a*), a bi-direction switching (i.e. switching can occur from the high state to the low state and from the low state to the high state for the same set of parameters) occurs only

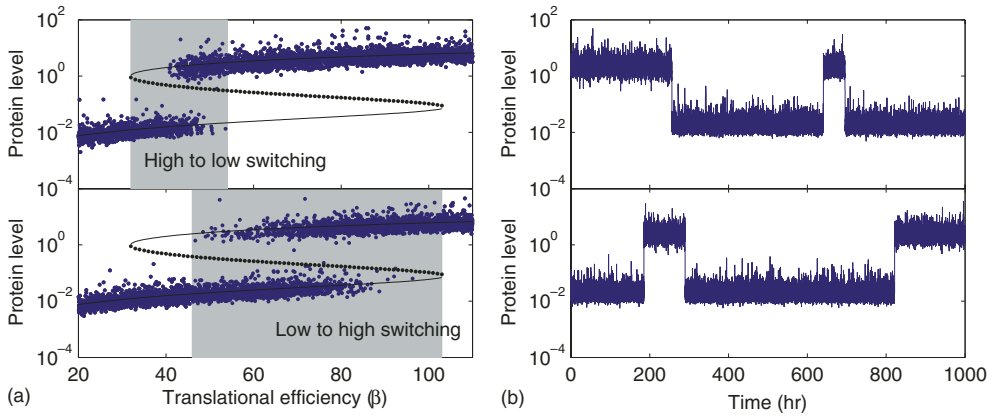

Figure 3. (*a*) Distribution of the cell states at 10 h as a function of the mean translational efficiency. Lower panel: each cell in this group is initially at the low state; upper panel: each cell is initially at the high state. (*b*) Two sample solutions that initiate from low state (low panel) and high state (upper panel), respectively. The parameters in the simulation are $\rho_0 = 0.006, \alpha = 0.0625, \theta_0 = 1.0, n_0 = 2, \tau_x = 50\,\text{s}, \tau_y = 50\,\text{s}, \tau_0 = 10\,\text{s}, \sigma = 1.0$ and $\beta = 50$ in (*b*).

when $46 < \beta < 54$. In a real biological system, the cell stays at one state for a significant period of time before switching to another state [20, 41, 50]. To be consistent with this, the master gene level should not switch too frequently from one state to another state. This requirement leads to a very tight range of β as indicated by our numerical simulations. For example, if we require the fractions of cells staying at least 10 h at one state is larger than 90%, then β has to be limited to a small neighbourhood around 50. Figure 3(*b*) shows two sample solutions with $\beta = 50$, initiating from the low or the high state.

In figure 3, the noise amplitude $\sigma = 1.9$, which corresponds to a very large noise effect on the translation efficiency. For this value, the standard deviation of the translational efficiency divided by its mean (often referred to as *coefficient of variance*) is 4.3, a number much larger than the experimentally measured normal fluctuation in gene expression [14, 46]. For example, in this case the probability of reducing the translational efficiency to 1/10 of its original mean value is larger than 38%, which is unrealistic.

In summary, in the system with only a positive feedback loop, we find bi-directional switching occurs only when σ is very large and β is well tuned in a very narrow range as seen in figure 3. In other words, the bistable switching observed in the system with only a positive feedback is not robust at all.

3.2. A negative feedback with a delay can destabilize the high state

Next, we consider the full model in figure 1. First, like the system without a negative feedback with delay we study the steady state (x^*, y^*) of the system, which satisfies the following equations:

$$y^* = \alpha h_0(\beta y^*) h_1(\beta y^*) \qquad x^* = \beta y^*. \tag{7}$$

The stability of the steady state (x^*, y^*) is determined by the characteristic equation [18]

$$h(\lambda) := \lambda^2 + c\lambda - a - b\mathrm{e}^{-\lambda\tau} = 0, \tag{8}$$

where

$$a = \frac{1}{\tau_x \tau_y}(\alpha\beta h_0'(x^*)h_1(x^*) - 1),$$

$$b = \frac{1}{\tau_x \tau_y}\alpha\beta h_0(x^*)h_1'(x^*), \qquad c = \frac{\tau_x + \tau_y}{\tau_x \tau_y}.$$

The steady state is stable if and only if all roots for (8) have negative real parts [18].

It is easy to show that when the delay $\tau = 0$, the eigenvalues are given by

$$\lambda_{1,2} = \frac{-c \pm \sqrt{c^2 + 4(a+b)}}{2}.$$

Since $c > 0$, the steady state is stable if and only if $a + b < 0$.

When $\tau > 0$ and the condition $a + b < 0$ is satisfied, we will show further that if and only if

$$a^2 - b^2 < 0, \tag{9}$$

there exists a critical delay $\tau_{\text{crit}} > 0$ such that the steady state is unstable when $\tau > \tau_{\text{crit}}$.

When $\tau = 0$, the condition $a + b < 0$ implies all roots of (8) have negative real parts. When $\tau > 0$, as τ increases from zero, the real parts of the roots change continuously with respect to the system parameters. Thus, the critical value of the parameters is determined by the condition by which one root of (8) has zero real part, i.e. (8) has a root of the form $\lambda = \mathrm{i}\omega$. Let $\lambda = \mathrm{i}\omega$ ($\omega > 0$), then (8) is equivalent to

$$\begin{aligned} &-\omega^2 - a - b\cos\omega\tau = 0, \\ &c\omega + b\sin\omega\tau = 0. \end{aligned} \tag{10}$$

Thus, ω satisfies

$$\omega^4 + (2a + c^2)\omega^2 + (a^2 - b^2) = 0. \tag{11}$$

Note that $h_0'(x^*) > 0$, it is easy to see

$$2a + c^2 = \frac{2\alpha\beta h_0'(x^*)h_1(x^*)}{\tau_x \tau_y} + \frac{\tau_x^2 + \tau_y^2}{(\tau_x \tau_y)^2} > 0.$$

Thus, equation (11) has a positive solution ω^2 if and only if (9) is satisfied, and the corresponding ω is given by

$$\omega = \sqrt{\frac{\sqrt{4ac^2 + c^4 + 4b^2} - (2a + c^2)}{2}}. \tag{12}$$

Substituting (12) into (10), we obtain the critical delay

$$\tau_{\text{crit}} = \frac{\cos^{-1}[-\dfrac{\sqrt{4ac^2 + c^4 + 4b^2} - c^2}{2b}]}{\sqrt{\dfrac{\sqrt{4ac^2 + c^4 + 4b^2} - (2a + c^2)}{2}}}. \tag{13}$$

Note that condition (9) ensures $0 < -\frac{\sqrt{4ac^2+c^4+4b^2}-c^2}{2b} < 1$, consequently $\tau_{\text{crit}} > 0$. Thus, from the above discussion, the steady state is stable when $0 < \tau < \tau_{\text{crit}}$, and unstable when $\tau > \tau_{\text{crit}}$. The critical delay time τ_{crit}, which depends on other parameters in the system, is essential in destabilizing the steady states. Similarly, condition (9) depends on the system parameters as well as the protein concentration at steady state, and the low state steady state

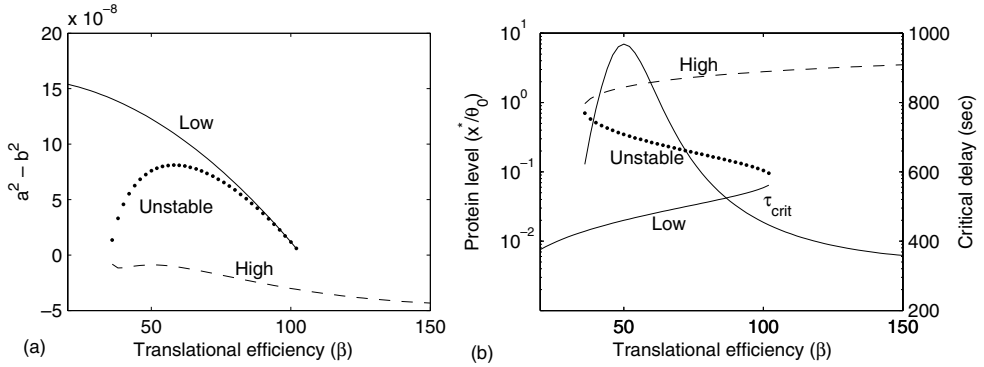

Figure 4. (*a*) The value $a^2 - b^2$ as a function of β and the protein level x^* at steady state. (*b*) The protein level (x^*/θ_0) at steady state and the critical delay τ_{crit} of the high state at different values of the translational efficiency β. In the simulation, $\rho_1 = 0.1, n_1 = 2$, and $\theta_1 = 2.5$ and other parameters are the same as those in figure 3.

does not satisfy condition (9) (see more discussion below). Figure 4(*a*) plots $a^2 - b^2$ as a function of β and the protein level x^*. In figure 4(*b*) the normalized protein level (x^*/θ_0) at steady state and the critical delay τ_{crit} for the high state are plotted at different values of β.

Here are some remarks on the existence of the critical delay:

(i) Condition (9) together with $a + b < 0$ yields

$$b < a < -b, \tag{14}$$

which automatically implies $b < 0$, i.e. $h_1'(x_*) < 0$. This condition indicates the importance of the negative feedback in the system figure 1.

(ii) In condition (14), the relationship $b < a$ means

$$\alpha\beta h_0(x^*)h_1'(x^*) < \alpha\beta h_0'(x^*)h_1(x^*) - 1,$$

which implies

$$\frac{1}{x^*} < \frac{h_0'(x^*)}{h_0(x^*)} - \frac{h_1'(x^*)}{h_1(x^*)} \tag{15}$$

by (7). If the low state satisfies $x^* \ll \min\{\theta_0, \theta_1\}$, we have in approximation

$$\frac{h_0'(x^*)}{h_0(x^*)} - \frac{h_1'(x^*)}{h_1(x^*)} \approx \frac{1}{x^*}\left(n(1-\rho_0)\left(\frac{x^*}{\theta_0}\right)^{n_0} + n(1-\rho_1)\left(\frac{x^*}{\theta_1}\right)^{n_1}\right) = o\left(\frac{1}{x^*}\right).$$

Thus, condition (15) is not satisfied for this case. As a result, the low state is unlikely to be unstable. However, condition (15) can easily be satisfied at the high state since the $1/x^*$ is a small value for this case, as seen in figure 4(*a*).

(iii) A similar characteristic equation like (8) was previously studied for a model of instantaneous damping with a delayed restoring force [13]. Following [13] to obtain a positive solution ω^2, one needs to require one of the following: (1) $a^2 - b^2 < 0$; (2) $a^2 - b^2 \geqslant 0$ and $2a + c^2 < 0$; or (3) $2b + c^2 = 0$ and $2a + c^2 < 0$. However, in the present system we always have $2a + c^2 > 0$, leading to condition (9).

All the analyses shown above suggest that the high state in a bistable system can be destabilized by the added negative feedback regulation and a delay in the feedback further amplify such a destabilization effect.

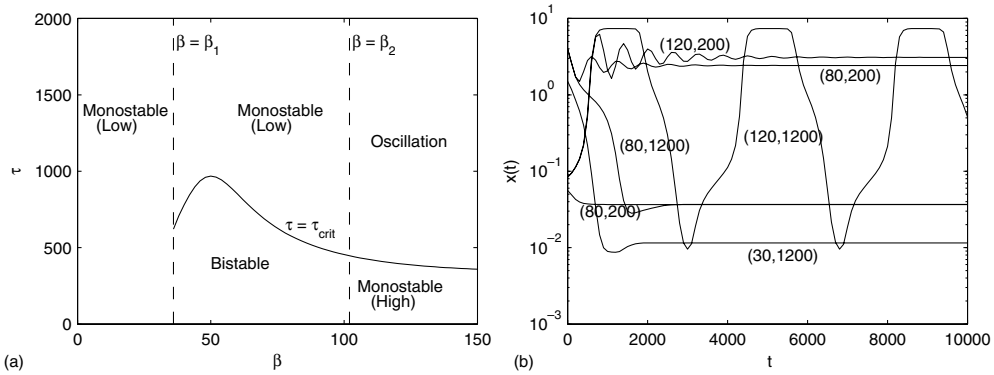

Figure 5. (*a*) Regions of stability in the (β, τ) plan; (*b*) example of the deterministic solutions for different values (β, τ), shown in the figure. The other parameters are the same as those in figure 4.

3.3. Dynamics of bi-directional switching

Based on the analysis, there exist two critical values $\beta_1 < \beta_2$ for the translational efficiency β and a critical delay τ_{crit} curve that divide the parameter plane β–τ into five regions (figure 5(*a*)). In particular, in the absence of noise, the dynamics of the system can be summarized as follows:

(i) If $\beta < \beta_1$, there is only one steady state (low state) and it is stable.
(ii) If $\beta_1 < \beta < \beta_2$ and $\tau < \tau_{\text{crit}}$, there are three steady states, among which the low and the high states are stable, and the intermediate state is unstable.
(iii) If $\beta_1 < \beta < \beta_2$ and $\tau > \tau_{\text{crit}}$, there are three steady states, among which the low state is stable, and the other two states (intermediate and high) are unstable.
(iv) If $\beta > \beta_2$ and $\tau < \tau_{\text{crit}}$, there is one steady state (high) and it is stable.
(v) If $\beta > \beta_2$ and $\tau > \tau_{\text{crit}}$, there is one steady state (high) and it is unstable, and the solutions are oscillatory.

Figure 5(*b*) shows the example solutions for different values of β and τ.

In the presence of noise, the region of interest is $\beta_1 < \beta < \beta_2$ and $\tau > \tau_{\text{crit}}$, in which bi-directional switching is possible. In this case, the two steady states, low state (x^*_{low}) and high state (x^*_{high}) are well defined, which are roots of the equation

$$\alpha h_0(x^*)h_1(x^*) - \beta x^* = 0.$$

When the solution is initially at the low state, and the noise may induce the switches to the high state as we have seen in previous simulations (figure 2). Assume the switching occurs around $t = t_0$, note that $x(t_0 - \tau) = x^*_{\text{low}}$, the protein level $x(t)$ does not reach the steady state x^*_{high} at t_0 immediately after the switch, but approaches a transition state x^*_{tran} that is approximately governed by the equation

$$\alpha h_0(x^*_{\text{tran}})h_1(x^*_{\text{low}}) - \beta x^*_{\text{tran}} = 0. \tag{16}$$

And $y(t)$ approaches $y^*_{\text{tran}} = x^*_{\text{tran}}/\beta$. Here x^*_{tran} is the maximum positive root of equation (16). In particular, if $x^*_{\text{low}} \ll \theta_1$, i.e. the negative feedback is off at the low state, then $h_1(x^*_{\text{low}}) \approx 1$ and hence x^*_{tran} is just the high state of the system without the negative feedback (figure 2).

Once switched, we will show that the solution $x(t)$ does not switch back to the low state during the time period $t_0 < t < t_0 + \tau$. When $t > t_0$, the deterministic solution is governed

approximately by the equations

$$\begin{aligned}
\tau_y \frac{\mathrm{d}x}{\mathrm{d}t} &= \beta y - x, \\
\tau_x \frac{\mathrm{d}y}{\mathrm{d}t} &= \alpha h_0(x) h_1(x_\tau) - y, \\
x(t) &= x^*_{\mathrm{low}} \quad (t < t_0), \\
x(t_0) &= x^*_{\mathrm{tran}}, \qquad y(t_0) = y^*_{\mathrm{tran}}.
\end{aligned} \tag{17}$$

When $t_0 < t < t_0 + \tau$, (17) can be written as

$$\begin{aligned}
\tau_y \frac{\mathrm{d}x}{\mathrm{d}t} &= \beta y - x, \\
\tau_x \frac{\mathrm{d}y}{\mathrm{d}t} &= \alpha h_1(x^*_{\mathrm{low}}) h_0(x) - y, \\
x(t_0) &= x^*_{\mathrm{tran}}, \qquad y(t_0) = y^*_{\mathrm{tran}}.
\end{aligned} \tag{18}$$

Consider equation (18), the steady state $(x^*_{\mathrm{tran}}, y^*_{\mathrm{tran}})$ is stable based on the discussion above. Therefore, the solution of (18) remains at the high state with $x(t)$ around x^*_{tran}. In particular, the solution of (17) will not switch back to the low state during $t_0 < t < t_0 + \tau$.

When $t = t_0 + \tau$, $x(t_\tau)$ switches to x^*_{tran}, and equation (18) is not valid for $t \geqslant t_0 + \tau$. On the other hand, the deterministic solution is governed by the equations

$$\begin{aligned}
\tau_y \frac{\mathrm{d}x}{\mathrm{d}t} &= \beta y - x, \\
\tau_x \frac{\mathrm{d}y}{\mathrm{d}t} &= \alpha h_0(x) h_1(x_\tau) - y, \\
x(t) &= x^*_{\mathrm{tran}} \qquad (t_0 < t \leqslant t + \tau), \\
y(t + \tau) &= y^*_{\mathrm{tran}}
\end{aligned} \tag{19}$$

when $t > t + \tau$. Since the delay $\tau > \tau_{\mathrm{crit}}$, the high state is unstable. Equation (19) has only one stable steady state, the low state, the solution will switch back to the low state at some time after $t_0 + \tau$.

In short, the analysis above suggests the following underlying mechanism for a noise-induced bi-directional switching. First, a cell at the low state may switch to the high state due to noise perturbation in the expression efficiency and bistability (due to the positive feedback loop) of the system. Once switched, the cell at the high state stays stable for a period of time due to the delay of the negative feedback loop in the system. And then, the high state becomes unstable once the effect of the negative feedback kicks in, and the cell switches back to the low state.

To test this mechanism, we numerically simulate a case with noise in which $\beta = 60$, and other parameters are the same as those in figure 3(*b*), i.e. no high to low state switching occurs, but add the negative feedback with a delay. To make the delay work, we choose the delay $\tau = 2$ h, which is larger than the critical $\tau_{\mathrm{crit}} \approx 1000$ s as seen in figure 4. Figure 6 shows the dynamics of protein level (x^*/θ_0) of 20 independent sample solutions, with each starting from the low state or the high state, for 50 h. As seen in figure 6, each solution switches between the two well-separated states: the low state with $0 < x^*/\theta_0 < 0.2$ and the high state with $x^*/\theta_0 > 1.0$. It can be seen that once the cell switches to the high state, it remains at the high state for about 4.3 h before switching back to the low state. How long does a cell stay at the low state or the high state? In general, how frequently does a cell switch? Next, we will study how switching frequency of a cell depends on some of the key system parameters.

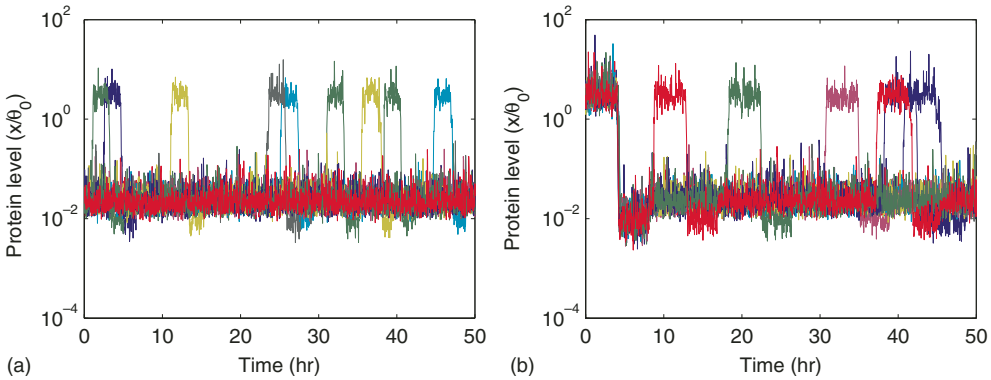

Figure 6. Bi-directional switching induced by noises. Time course of 20 independent solutions with each starting from (*a*) the low state or (*b*) the high state, respectively. Here, $\beta = 60$, $\tau = 7200$ and the other parameters are the same as in figure 3 and 4.

3.4. Switching frequency

Switching frequency is a quantity often measured in experiment to study the capability of a cell to switch from one state to other state under different genetic conditions [35]. One may estimate the switching frequency of a cell in the following way. Assume that the solution $x(t)$ of a cell initially is at the low state. Define $\{t_i\}$ and $\{s_i\}$ to be two time series as

$$t_i = \min\{t | t > s_{i-1}, x(t) \text{ reaches the high state}\} \tag{20}$$

and

$$s_i = \min\{s | s > t_i, x(s) \text{ reaches the low state}\}. \tag{21}$$

It is easy to have

$$0 = s_0 < t_1 < s_1 < t_2 < s_2 < \cdots.$$

Then, the duration time (lifetime) of the solution (cell) staying at the high state and the low state can be estimated by the two time series

$$T^i_{\text{high}} = s_i - t_i \qquad (i = 1, 2, \ldots)$$

and

$$T^i_{\text{low}} = t_i - s_{i-1}, \qquad (i = 1, 2, \ldots),$$

respectively. So the averaging of the above time intervals

$$T_{\text{high}} = \lim_{n\to\infty} \frac{1}{n} \sum_{i=1}^{n} T^i_{\text{high}} \tag{22}$$

and

$$T_{\text{low}} = \lim_{n\to\infty} \frac{1}{n} \sum_{i=1}^{n} T^i_{\text{low}} \tag{23}$$

are natural estimation of the average lifetimes of the high state and the low state, respectively.

First, we vary τ to study how T_{high} depends on τ. As seen in figure 7(*a*), the average lifetime of the high state is linearly correlated with the delay τ. In particular, the numerically estimated average lifetime of a cell can be fitted by the following linear relation:

$$T_{\text{high}} = 1.90\tau + 0.35(\tau > \tau_{\text{crit}}). \tag{24}$$

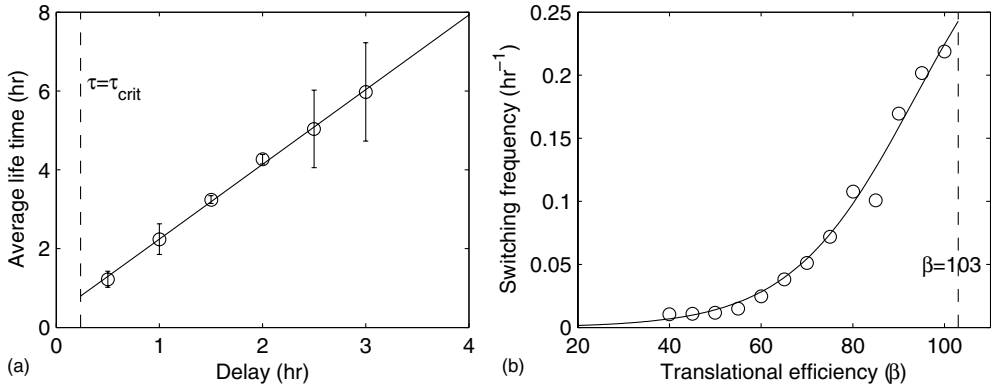

Figure 7. (*a*) Average lifetime of high state as a function of delay τ. (*b*) Dependence of frequency for switching from low to high on β. Circles are from the direct simulations and solid curves are data fitting. Other parameters in the simulation are the same as in figure 6.

Such a linear relationship is expected from our analysis in the previous sections since the stability of the high state is mainly affected by the negative feedback and the timing of such an effect is dictated by the delay constant τ.

Unlike the high to low switching, which is affected by deterministic factors, the switching from the low to high is mainly driven by noises. Thus, the lifetime of the low state should depend on noise and its interactions with other parameters in the system. Assume that the lifetime $\{T^i_{\text{low}}\}$ is the Poisson distributed and let p be the probability that a cell switches from the low to the high state within 1 h, then the probability of $T^i_{\text{low}} = n$ hours is given by $(1-p)^{n-1}p$. The average lifetime for the cell at the low state becomes

$$T_{\text{low}} = \sum_{n>0} n(1-p)^{n-1}p = 1/p. \tag{25}$$

Thus, the switching frequency, or the probability of the switching, is $p = 1/T_{\text{low}}$. Figure 7(*b*) shows the dependence of switching frequency on the translational efficiency β. The switching frequency is an increasing function of β, as expected, and the relationship can be well fitted by a sigmoid function

$$p = \frac{0.36}{1 + \mathrm{e}^{-(\beta - 93.3)/13.5}} \qquad (\beta < 103). \tag{26}$$

Here the low to high switch is meaningful only when the low state is stable in the absence of noise. Thus, function (26) is valid only when $\beta < 103$ according to the bifurcation diagram shown in figure 2. Of course, the details in the fitting form (24) and (26) depend on other parameters, the general trend of dependence remains similar.

In general, the switching frequency from the high to the low state is determined by the delay of the negative feedback, and the frequency of the switching from the low to the high state is determined by the noise and translational efficiency. For example, from (26), if $13.8 < \beta < 45.3$, then the switching frequency is between $0.001 < p < 0.01\,(\text{h}^{-1})$. The range of parameters ensuring the bi-directional switching in the presence of a negative feedback is usually much larger than the system without a negative feedback.

4. Discussion

In this paper, we have studied noise-induced switching using a model consisting of a positive feedback and a negative feedback with a time delay. Similar to other switching systems, the positive feedback loop is responsible for creating bistability that is necessary for switching. The time delay in the negative feedback has been found to be critical to induce robust bi-directional switching, that is the system can robustly switch from one state to another back and forth under the same set of parameters. In particular, the negative feedback in the system mainly functions to destabilize the high state and the time delay allows the system staying for a period of time at the high state. Negative feedbacks with delay were previously found in other gene regulation networks to induce oscillations [27, 31].

Our model provides a simple mechanism for bi-directional switching induced by noise. Clearly, in real biological systems, the biochemical machinery responsible for bistability may be much more complex than just a simple positive feedback loop. For example, double-negative feedbacks exist in the toggle switch and there are double-negative feedbacks in addition to positive feedback loops in white-opaque switching in *Candida albicans*. Our framework should be able to include those detailed regulations in a straightforward way, and similar results are expected. The time delay in feedback loops has been observed in many biological systems [8, 24, 27, 30, 31]. Such time delay may come from transcription and translation of mRNAs and proteins in many regulations that exhibit an overall effect of a negative feedback in regulating the master gene, or from the master gene's interaction with other pathways in the system. Anyway, it would be interesting to experimentally search for and identify such negative regulations in real biological systems to study their effect on switching, for example, through mutations on the components required for the negative feedback loops to remove the negative feedback regulation.

Switching frequency, which may be estimated experimentally by counting the number of cells at different cell states during a time course [35], is an important quantity that can be used to characterize stability of different cell fates. While many modelling studies have been conducted to figure out whether a system allows switching, little work exists on study of how likely a system switches. By comparing switching frequency obtained through modelling with those measured by experiments, we may find limitation of one model and advantage of another, potentially leading to prediction of new regulations for experimental testing. For a biological system switching between two states, a good model for the system should not only exhibit bistability but also need to capture the switching frequency of the real biological system.

Acknowledgments

JL is supported by the National Science Foundation of China (NSFC 1061029). QN is supported by NIH grants R01GM75309, R01GM67247, P50GM76516 and NSF grant DMS-0917492. QN would like to dedicate this work to Professor Todd Dupont for his inspiration, guidance and mentoring when QN was a Dickson instructor at the University of Chicago from 1997 to 1999.

References

[1] Acar M, Mettetal J T and van Oudenaarden A 2008 Stochastic switching as a survival strategy in fluctuating environments *Nature Genet.* **40** 471–5

[2] Alon U 2007 *An Introduction to Systems Biology* (London: Chapman and Hall/CRC)

[3] Atkinson M R, Savageau M A, Myers J T and Ninfa A J 2003 Development of genetic circuitry exhibiting toggle switch or oscillatory behavior in *Escherichia coli*. *Cell* **113** 597–607

[4] Austin D W, Allen M S, McCollum J M, Dar R D, Wilgus J R, Sayler G S, Samatova N F, Cox C D and Simpson M L 2006 Gene network shaping of inherent noise spectra *Nature* **439** 608–11

[5] Barik D, Paul M R, Baumann W T, Cao Y and Tyson J J 2008 Stochastic simulation of enzyme-catalyzed reactions with disparate time scales *Biophy. J.* **95** 3563–74

[6] Becskei A, Séraphin B and Serrano L 2001 Positive feedback in eukaryotic gene networks: cell differentiation by graded to binary response conversion *EMBO J.* **20** 2528–35

[7] Bennett R and Johnson A 2005 Mating in *Candida albicans* and the search for a sexual cycle *Annu. Rev. Microbiol.* **59** 233–55

[8] Bratsun D, Volfson D, Tsimring L S and Hasty J 2005 Delay-induced stochastic oscillations in gene regulation *Proc. Natl Acad. Sci. USA* **102** 14593–8

[9] Cherry J L and Adler F R 2000 How to make a biological switch *J. Theor. Biol.* **203** 117–33

[10] Chen K C, Calzone L, Csikasz-Nagy A, Cross F R, Novak B and Tyson J J 2004 Integrative analysis of cell cycle control in budding yeast *Mol. Biol. Cell.* **15** 3841–62

[11] Chou C, Zhang Y, Zhao R and Nie Q 2007 Numerical methods for stiff reaction–diffusion systems *Discrete Contin. Dyn. Syst.* B **7** 515–25

[12] Conrad E, Mayo A E, Ninfa A J and Forger D B 2008 Rate constants rather than biochemical mechanism determine behavior of genetic clocks *J. R. Soc. Interface* **5** S9–15

[13] Cooke K L and Grossman Z 1982 Discrete delay, distributed delay and stability switches *J. Math. Anal. Appl.* **86** 592–627

[14] Elowitz M B, Levine A J, Siggia E D and Swain P S 2002 Stochastic gene expression in a single cell *Science* **297** 1183–6

[15] Ferrell J E Jr 2002 Self-perpetuating states in signal transduction: positive feedback, double-negative feedback and bistability *Curr. Opin. Chem. Biol.* **6** 140–8

[16] Gardner T S, Cantor C R and Collins J J 2000 Construction of a genetic toggle switch in *Escherichia coli*. *Nature* **403** 339–42

[17] Golding I, Paulsson J, Zawilski S M and Cox E C 2005 Real-time kinetics of gene activity in individual bacteria *Cell* **123** 1025–36

[18] Hale J 1977 *Theory of Functional Differential Equations* (Berlin: Springer)

[19] Hasty J, Pradiness J, Dolnik M and Collins J J 2000 Noise-based switches and amplifiers for gene expression *Proc. Natl Acad. Sci. USA* **97** 2075–80

[20] Huang G, Wang H, Chou S, Nie X, Chen J and Liu H 2006 Bistable expression of WOR1, a master regulator of white-opaque switching in *Candida albicans*. *Proc. Natl Acad. Sci. USA* **103** 12813–18

[21] Kaufmann B B, Yang Q, Mettetal J T and van Oudenaarden A 2007 Heritable stochastic switching revealed by single-cell genealogy *PLoS Biol.* **5** e239

[22] Kaufmann B B and van Oudenaarden A 2007 Stochastic gene expression: from single molecules to the proteome *Curr. Opin. Genet. Dev.* **17** 107–12

[23] Kærn M, Elston T C, Blake W J and Collins J J 2005 Stochasticity in gene expression: from theories to phenotypes *Nature Rev. Genet.* **6** 451–64

[24] Kerszberg M 2004 Noise, delays, robustness, canalization and all that *Curr. Opin. Genet. Devices* **14** 440–5

[25] Kvaal C, Lachke S A, Srikantha T, Daniels K, McCoy J and Soll D R 1999 Misexpression of the opaque-phase-specific gene PEP1 (SAP1) in the white phase of *Candida albicans* confers increased virulence in a mouse model of cutaneous infection *Infect. Immun.* **67** 6652–62

[26] Lei J 2009 Stochasticity in single gene expression with both intrinsic noise and fluctuation in kinetic parameters *J. Theor. Biol.* **256** 485–92

[27] Lewis J 2003 Autoinhibition with transcriptional delay: a simple mechanism for the zebrafish somitogenesis oscillator *Curr. Biol.* **13** 1398–408

[28] Maamar H and Dubnau D 2005 Bistability in the *Bacillus subtilis* K-state (competence) system requires a positive feedback loop *Mol. Microbiol.* **56** 615–24

[29] Maheshri N and O'Shea E K 2007 Living with noisy genes: how cells function reliably with inherent variability in gene expression *Annu. Rev. Biophys. Biomol. Struct.* **36** 413–34

[30] Monk N 2003 Oscillatory expression of Hes1, p53, and NF-κ B driven by transcriptional time delays *Curr. Biol.* **13** 1409–13

[31] olde Scheper T, Klinkenberg D, Pennartz C and van Pelt J 1999 A mathematical model for the intracellular circadian rhythm generator *J. Neurosci.* **19** 40–7

[32] Ozbudak E M, Thattai M, Lim H N, Shraiman B I and van Oudenaarden A 2004 Multistability in the lactose utilization networks of *Escherichia coli*. *Nature* **427** 737–40

[33] Paulsson J 2004 Summing up the noise in gene networks *Nature* **427** 415–8
[34] Raj A and van Oudenaarden A 2008 Nature, nurture, or chance: stochastic gene expression and its consequences *Cell* **135** 216–26
[35] Rikkerink E H, Magee B B and Magee P T 1988 Opaque-white phenotype transition: a programmed morphological transition in *Candida albicans J. Bacteriol.* **170** 895–9
[36] Schaffer W M 1974 Optimal reproductive effort in fluctuating environments *Am. Naturalist.* **108** 783–90
[37] Samoilov M S, Price G and Arkin A P 2006 From fluctuations to phenotypes: the physiology of noise *Sci. STKE* **2006** re17
[38] Santillán M and Mackey M C 2008 Quantitative approaches to the study of bistability in the lac operon of *Escherichia coli*. *J. R. Soc. Interface* **5** S29–39
[39] Shahrezaei V, Ollivier J F and Swain P S 2008 Colored extrinsic fluctuations and stochastic gene expression *Mol. Syst. Biol.* **4** 1–9
[40] Shahrezaei V and Swain P S 2008 The stochastic nature of biochemical networks *Curr. Opin. Biotechnol.* **19** 369–74
[41] Slutsky B, Staebell M, Anderson J, Risen L, Pfaller M and Soll D R 1987 'White-opaque transition': a second high-frequency switching system in *Candida albicans*. *J. Bacteriol.* **169** 189–97
[42] Soll D R, Morrow B and Srikantha T 1993 High-frequency phenotypic switching in *Candida albicans Trends Genet.* **9** 61–5
[43] Soll D R 1997 Gene regulation during high-frequency switching in *Candida albicans*. *Microbiology* **143** 279–88
[44] Sriram K, Soliman S and Fages F 2009 Dynamics of the interlocked positive feedback loops explaining the robust epigenetic switching in *Candida albicans*. *J. Theor. Biol.* **258** 71–88
[45] Stearns S C 1976 Life-history tactics: a review of the ideas *Quart. Rev. Biol.* **51** 3–7
[46] Swain P S, Elowitz M B and Siggia E D 2002 Intrinsic and extrinsic contributions to stochasticity in gene expression *Proc. Natl Acad. Sci. USA* **99** 12795–800
[47] Tian T and Burrage K 2006 Stochastic models for regulatory networks of the genetic toggle switch *Proc. Natl Acad. Sci. USA* **103** 8372–7
[48] Tsuboi R *et al* 1994 Pathogenesis of superficial mycoses *J. Med. Vet. Mycol. (Suppl.)* **32** 91–104
[49] Veening J, Smits W K and Kuipers O P 2008 Bistability, epigenetics, and bet-hedging in bacteria *Annu. Rev. Microbiol.* **62** 193–210
[50] Wang L, Walker B L, Iannaccone S, Bhatt D, Kennedy P J and Tse W T 2009 Bistable switches control memory and plasticity in cellular differentiation *Proc. Natl Acad. Sci. USA* **106** 6638–43
[51] Yan G, Lee T J, Mori S, Nevins J R and You L 2008 A bistable Rb-E2F switch underlies the restriction point *Nature Cell Biol.* **10** 476–82
[52] Zordan R E, Galgoczy D J and Johnson A D 2006 Epigenetic properties of white-opaque switching in *Candida albicans* are based on a self-sustaining transcriptional feedback loop *Proc. Natl Acad. Sci. USA* **103** 12807–12